Arabian Journal for Science and Engineering (2021) 46:6207–6217
https://doi.org/10.1007/s13369-020-04897-6

RESEARCH ARTICLE-CHEMICAL ENGINEERING

Silsesquioxanes-Based Nanolubricant Additives with High Thermal Stability, Superhydrophobicity, and Self-cleaning Properties

Numan Ahmed[1] · Xianwei Zhang[1] · Shah Fahad[1] · Muhammad Imran Jamil[2] · Tariq Aziz[1] · E. Husamelden[1] · Carla Bittencourt[3] · Jintao Wan[4] · Hong Fan[1]

Received: 21 January 2020 / Accepted: 18 August 2020 / Published online: 3 September 2020

Abstract

Nanoadditives are promising materials for long-envisioned next-generation lubricants to achieve excellent tribological performance and thermal stability. Here, an instigative and novel approach has been scrutinized to facilely prepare the nanolubricant additive. For this purpose, three synthetic strategies were designed for i) preparation of uniform-sized poly(methyl silsesquioxane) (PMSQ) nanoparticles, ii) hydrosilylation of the long carbon chain of ethyl 10-undecenoate and iii) modification of PMSQ nanoparticles with hydrosilylation product through a condensation reaction, in order to obtain long-carbon-chain grafted nanohybrids. The morphology, composition, and properties of these nanohybrids were confirmed by ^{1}H-NMR, FTIR, SEM, EDS, and TGA. The effects of different concentrations of unmodified and modified PMSQ nanoparticles on the tribological properties of silicone oil were discussed. In the comparison of unmodified PMSQ nanoparticles, the modified one performs very well to reduce the coefficient of friction and wear scar diameter at low concentration. The TGA results revealed the extraordinary thermal stability of these particles, as their weight loss was only 19% at 800 °C which is remarkably higher than other solid lubricant additives. In this research, we tried to fill the deficiency of thermally stable material in the field of heavy machinery and industry. In addition, the environment-friendly (fluorine-free), superhydrophobic and self-cleaning surface effect of modified PMSQ nanoparticles was also observed. These silsesquioxane-based nanohybrids having synergistic effects, advantageous scientific values, and promising application prospects are expected to be more useful with other longer carbon chains.

Keywords Nanohybrids · Solid lubricant additive · Thermal stability · Hydrosilylation · Tribological performance · Self-cleaning

1 Introduction

For hundreds of years, mankind has been making efforts to reduce the friction from appliances of their daily life usage. It is a fundamental phenomenon in nature and can be observed everywhere. The use of lubricants is a common way to reduce the friction, energy dissipation and improve the performance of the material. On every frictional surface, there are always some nano- and micrometer-sized peaks and grooves that act as the originator of friction. To overcome friction, different liquid and solid lubricants are normally used for this purpose [1]. However solid lubricants and lubricating additives in oils, plastics, coatings, and grease are used for those environments where the harsh conditions are being implemented.

Electronic supplementary material The online version of this article (https://doi.org/10.1007/s13369-020-04897-6) contains supplementary material, which is available to authorized users.

✉ Hong Fan
hfan@zju.edu.cn

Numan Ahmed
numan.bs922@outlook.com

[1] State Key Laboratory of Chemical Engineering, College of Chemical and Biological Engineering, Zhejiang University, Zheda Road no. 38, Xihu District, Hangzhou 310027, China

[2] Zhejiang Provincial Key Laboratory of Advanced Chemical Engineering Manufacture Technology, College of Chemical and Biological Engineering, Zhejiang University, Zheda Road no. 38, Xihu District, Hangzhou 310027, China

[3] Centre of innovation and research in Materials and Polymers (CIRMAP), University of Mons, Place du Parc 23, B-7000 Mons, Belgium

[4] School of Materials science and Engineering, Shaanxi Normal University, Xi'an 710119, China

Over the liquid lubricants, solid lubricants have the capability to perform under high load, having high thermal stability and the diversity of the applications[2,3].

Solid nanolubricant additives have attracted much intention due to their small size and surface smoothening properties in different lubrication systems. Different materials of this kind are in practice for improving tribological performance i.e., inorganic lubricants like graphite, sulfides of tungsten, molybdenum, and gallium (WS_2, MoS_2GaS), boron nitride (BN), and borax ($Na_2B_4O_7$), some oxides such as MnO_2 and TiO_2, some soaps like calcium and sodium salts of fatty acids, and organic compounds like polychlorotrifluoroethylene (PCTFE) and polytetrafluoroethylene (PTFE), etc. [4–6].

In recent years, the prompt developments in nanotechnology make the hybrid nanomaterials an important choice as nanolubricant or lubricant additives in the field of tribology. The high-performance hybrid nanomaterials with improved functionalities were specifically designed to reduce the wear and friction, which have considerable potential applications in fluid flow, electronics, metallurgy, and automobile industry. In this area, literature encompasses several reports where different lubricants or lubricant additives have been investigated for evaluating their tribological performance. For example, Wu et al. used graphene oxide (GO) nanoparticles as an additive in aviation lubricant oil (4010 AL) and found that the performance of GO nanoparticles in friction improvement is higher at 0.5 wt% [2]. Lei et al. modified vinyl-terminated polyhedral oligomeric silsesquioxane (POSS) nanohybrids with 1-dodecanthiol (OS-POSS) and 1-octadecanethiol (OD-POSS) via "thiol-ene click" reaction. These modified POSS nanohybrids showed good performance to reduce wear scar diameter (WSD) and coefficient of friction (COF) [7]. Lu and co-workers prepared the WS_2 and WS_2/TiO_2 nanoparticles. They found that out of two types of nanoadditives, the WS_2/TiO_2 additives showed good anti-wear performance and the synergistic lubrication effect by improving the tribological performance of diisooctyl sebacate (DOS) [8]. Simic and his team prepared the inorganic fullerene-like tungsten disulfide (IF-WS_2) nanomaterial incorporated with poly(vinyl butyral) PVB. The performance of IF-WS_2/PVB was investigated by dissolving them in different solvents, and the analysis revealed that IF-WS_2/PVB composite in ethanol showed good improvement in friction reduction [9]. All these lubricant additives have good friction reduction efficiencies but insufficient thermal stabilities. As heavy industries required high thermally stable lubricants, to fill this gap and meet the demand, we made an innovation by using thermally robust silsesquioxanes and modify them with long carbon chains.

Recently, organosilica hybrids, i.e., polysilsesquioxanes (PSQs), obtained from different processes have attracted much attention owing to their ability to control the processability of the materials via the chemistry of organosilica by combining it with highly diverse organic functionalities [10,11]. These hybrid materials are quite famous as they exhibit unique properties, from their different inorganic and organic parts in a synergistic way. Various materials have become thermally stable, mechanically tough, highly hydrophobic, and bearer of good lubrication properties by incorporation of PSQs. Due to all these properties, this class of hybrid materials has become the most studied topic by researchers in the past decades [12,13].

Hydrophobic solid surfaces are very important in surface engineering, related to practical applications. Usually, these surfaces are prepared by fluorine-containing materials and long-alkyl-chain moieties having low surface energy [14,15], exhibiting higher contact angles. By following this streamline, superhydrophobic cotton was fabricated with fluoroalkylsiloxanes by Ivanova et al. [14] However, fluorine-containing compounds have serious problems for the environment as they are easy to accumulate in biological chains, difficult to degrade in nature, and harmful to the human body. That is why surface modification-related fluorine compounds have been listed in Annex B of the Stockholm Convention (SC) on Persistent Organic Pollutants (PoPs) [16,17]. Mainly two crucial factors are responsible for highly hydrophobic or superhydrophobic surfaces, i.e., the nature of the material (having fluorine and long carbon chain) and the rough surfaces that have a smaller fraction of surface area of solid–liquid drops than liquid–gas. So it expected that by the modification of nonfluorinated long alkyl chain on the surface of robust silsesquioxane particles, we can integrate the thermally stable lubricity and environmentally friendly superhydrophobicity in one material.

In this study, the novel uniform-sized long carbon chain containing hybrid poly(methyl silsesquioxanes) (PMSQs) with narrow-size-distribution, extraordinarily thermally stable, and moisture-protective superhydrophobic nanoparticles were prepared. The effect of different concentrations of unmodified PMSQ nanoparticles (P-NPs) and modified PMSQ nanoparticles (MP-NPs) in silicone oil was studied, and the change in wear scar diameter (WSD) as well as coefficient of friction (COF) was analyzed, which showed that MP-NPs surprisingly improved the tribological performance even at low concentration.

The main innovative point of this research is to prepare the extraordinarily thermally stable solid lubricant additive than already prepared ones, having good tribological performance. This material additionally showed the environmentally friendly (fluorine-free) superhydrophobicity and self-cleaning properties after embedded on the glass surface, which can enable it to protect the substrate from rust to moisture.

2 Experimental

2.1 Chemicals and Materials

Methyltriethoxysilane (MTES) (99% pure) and triethoxysilane (TES) (99% pure) were purchased from Energy Chemicals (China). Ethyl 10-undecenoate was purchased from Tokyo chemicals ltd. (98% pure), sodium dodecylbenzene sulfonate (SDBS) (92% pure) and hexachloroplatinic acid hexahydrate (Speier's catalyst) (99.9% pure) from Aladdin (Shanghai, China), and silicone oil (polydimethylsiloxane or dimethicone) (99% pure), hexamethylenetetramine (95% pure), ammonium hydroxide (28% v/v), and analytical-grade toluene, ethanol, acetone, sulfuric acid, hydrogen peroxide from Sino chemical reagents. Room-temperature-vulcanized (RTV) silicone adhesive was purchased from Shenzhen Xingyong Company.

2.2 Preparation of PMSQ Nanoparticles

PMSQ nanoparticles (P-NPs) were prepared by using a facile single-step sol–gel process in an aqueous medium. In this process, 24.9 g MTES was added in 270 mL water with 0.5 g SDBS under 800 rpm stirring speed for 30 min. SDBS is a good surfactant that prevents the particles to agglomerate and gives the fine size distribution after particle formation. After that, reaction was catalyzed with 0.45 mL ammonium hydroxide (28% v/v) by slow addition and thoroughly mixed with proper agitation. The reaction was allowed to continue at 30 °C for 12 h until the mixture turned into bright-white-color precipitates. Finally, the P-NPs were separated by centrifugal sedimentation and ultrasonic dispersion three times along with careful washing by ethanol and water and then dried in a vacuum oven at 80 °C for 10 h. After that, dried powder was further ground by a ball mill machine to obtain fine particles.

2.3 Hydrosilylation of Ethyl 10-undecenoate

For the hydrosilylation, 40 mL of toluene (pre-dried) was added in 250-mL three-neck flask under normal stirring speed and let the N_2 pass through for 15 min. to achieve inert environment. After that, 5.3 g (25.0 mmol) of ethyl 10-undecenoate and 0.8 mL of 80 mg/L hexachloroplatinic acid H_2PtCl_6 (0.08% solution in isopropanol) as a catalyst were poured into the flask, and 8.2 g (50.0 mmol) of triethoxysilane (ethyl 10-undecenoate and triethoxysilane molar ratio is 1:2) was added slowly by microinfusion pump in 4 h and then the reaction was allowed to proceed for further 14 h at 80^{o} C. Finally, the solvent and unreacted reactants were evaporated through the rotary evaporator and the resulted product ethyl 11-(triethoxysilyl)undecanoate (called S2E11, S2 from the second step and E11 from the first part of the name ethyl 11-(triethoxysilyl)undecanoate) was obtained.

2.4 Modification of P-NPs

The P-NPs were modified by simple chemical precipitation technique. For this, 5.0 g of P-NPs along with 0.75 g of S2E11 was ultrasonically dispersed in 100 mL mixture of ethanol and water (3:1) for 30 min. Then, it was poured into 250-mL flask and properly mixed for 15 min. with a 500 rpm stirring rate. To keep the pH of solution 9, the ammonium hydroxide was carefully added. Another solution of 1.90 g of hexamethylenetetramine into 25 mL deionized water was added drop by drop within 15 min. The solution was heated at 70 °C for 3 h by constant stirring. Finally, the reaction was stopped and let the solution cool and settle down for 2 h and the precipitates were centrifuged three times with ethanol and deionized water. The product was dried in a vacuum at 80 °C for 10 h. All the above-mentioned steps are shown in Scheme 1.

2.5 Fabrication of Superhydrophobic Surface

The smooth coating of MP-NPs on the glass surface was fabricated as follows: to get a clean glass surface first, the 2.5 cm × 2.5 cm microscopic glass slides were washed with acetone and sonicated for 10 min. For further high purity of surface, the glass slides were immersed in piranha solution (concentrated sulfuric acid + hydrogen peroxide with volume ratio 7:3), heated for 30 min., further washed with excess distilled water and dried in a blast furnace at 150 °C. The room-temperature-vulcanized (RTV) silicone adhesive as a binder was smoothly applied on the glass with a film applicator and dried at 40 °C for 10 min. The MP-NPs were dissolved in n-dodecane to make a solution form for easy spreading of particles on the adhesive surface. The MP-NPs coating was prepared by casting 1 ml of the solution onto the RTV layer, and finally n-dodecane was dried completely.

2.6 Characterization

The size distribution of P-NPs was determined by dynamic light scattering (DLS) technique at 25 °C by making a suspension in anhydrous ethanol using a 0.2 um Macherey–Nagel filter in Malvern Zetasizer Nano ZS, Malvern, UK, with HeNe lasers (633 nm). Before the measurements, samples were ultrasonicated for 30 min. to achieve homogeneity. ^{1}H-NMR was used to verify the hydrosilylation of ethyl-10-undecenoate using $CDCl_3$ as a solvent by 500 MHz (Bruker). Scanning electron microscope SEM-8010 (HITACHI Japan) was employed to determine the structure, roughness, and morphology of unmodified PMSQ nanoparticles (P-NPs) and MP-NPs. (Here, PMSQ nanoparticles (P-NPs) are also named as unmodified PMSQ nanoparticles in comparison with modified PMSQ nanoparticles (MP-NPs).) Modification of a long carbon chain on P-NPs was determined by

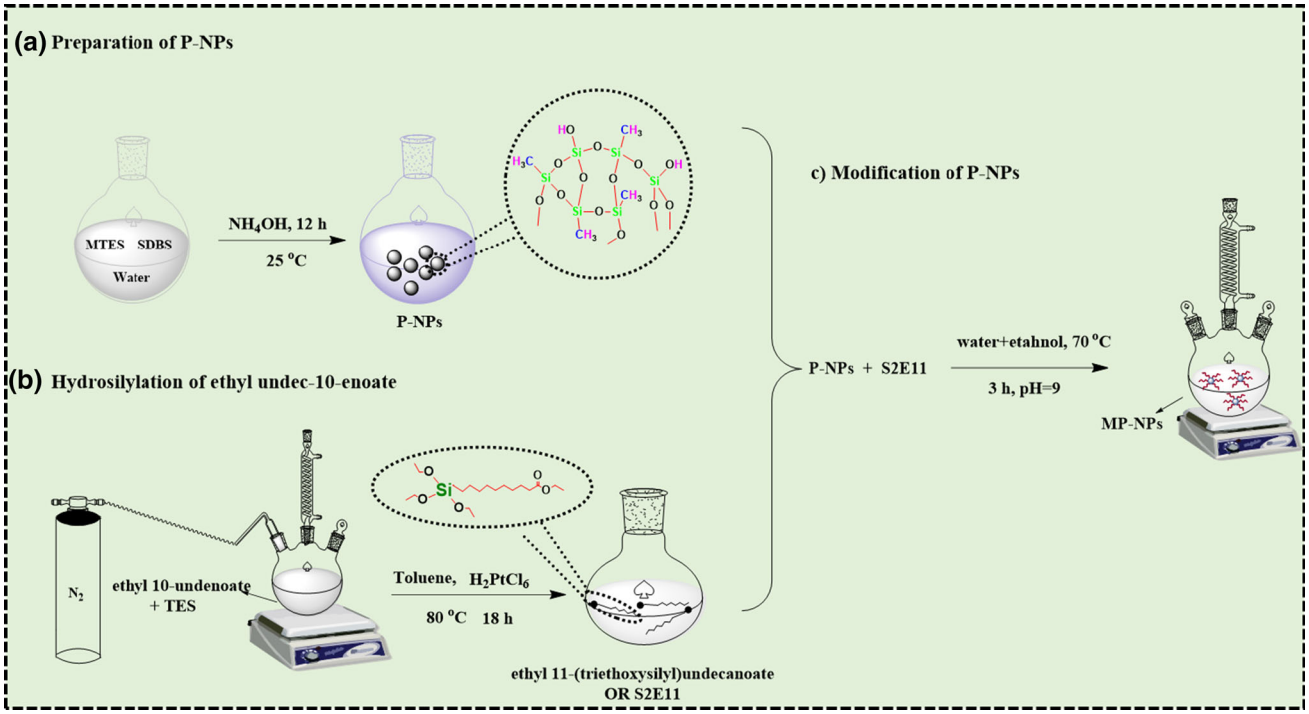

Scheme 1 Illustration of **a** preparation of P-NPs, **b** hydrosilylation of ethyl 10-undecenoate and **c** modification of P-NPs

Fourier transform infrared spectroscopy (FTIR, Nicolet 5700 Thermo Fisher Co.) in a KBr matrix. The percentage contents of each element were analyzed by energy-dispersive X-ray spectroscopy (EDS) with SEM measurement. Thermogravimetric analysis (TGA) was performed on TA instruments Q-500 at the heating rate of 10 °C min^{-1} under N_2 flow (250 mL min^{-1}) up to 800 °C. The lubrication performance of MP-NPs with various concentrations was evaluated by Natai four-ball friction tester. One steel ball sliding against three steel balls was used for measuring WSD and COF. The relation between concentration of MP-NPs and lubrication properties was further confirmed by EDS. The water contact angle (WCA) was measured by Data Physics OCA 20, USA, California, with 5 µl (sessile drop method) of distilled water. The average values were obtained by calculating the WCA in at least three different positions.

3 Results and Discussion

3.1 Hydrosilylation of Ethyl-10-undecenoate with TES

The hydrosilylation of ethyl-10-undecenoate was done by triethoxysilane (molar ratio 1:2) in the presence of toluene as a solvent and Speier's catalyst (H_2PtCl_6). After purification, a transparent light-yellowish-color oily product was obtained. The ^{1}H-NMR of ethyl-10-undecenoate and the hydrosilylation product ethyl 11-(triethoxysilyl)undecanoate (S2E11) is an evidence of successful hydrosilylation as shown in Fig. 1a, b.

For the ethyl-10-undecenoate ^{1}H-NMR, the signals at 1.15 ppm are attributed to methyl hydrogen atoms attached with methylene carbon which is further attached with the oxygen of carbonyl carbon (–COO–CH_2–CH_3). The detailed assignment of ^{1}H-NMR spectra (500 MHz, $CDCl_3$, δ ppm) is listed as follows: 1.15 (t, –COO–CH_2CH_3, 3), 1.22-1.32 (m, –$CH_2(CH_2)_5$–CH_2–CH_2–COO–, 10) 1.55 (p, –CH_2–CH_2–COO–, 2), 1.95 (q, CH_2 = CH–CH_2–, 2), 2.21 (t, –CH_2–COO–, 2), 4.12 (q, –COO–CH_2–CH_3, 2), 4.92 and 4.98 for one *cis*- and one *trans*-hydrogen (m, CH_2= CH-CH_2-, 2), 5.56 (m, CH_2 = C*H*–).

The hydrosilylation product ethyl 11-(triethoxysilyl)undecanoate (S2E11) ^{1}H-NMR (500 MHz, $CDCl_3$): δ ppm, 0.55 and 0.81 for one *cis*- and one *trans*-hydrogen (t, $(CH_3CH_2O)_3Si$–CH_2, 2), 1.12 (t, –COO–CH_2CH_3, 3), 1.18 (t, $(CH_3CH_2O)_3Si$–, 9), 1.21-1.32 (m, –$CH_2(CH_2)_7$–CH_2-CH_2–COO–, 14), 1.55 (t, –$(CH_2)_7$–CH_2–CH_2–COO–, 2), 2.21 (t, –CH_2–CH_2–COO–, 2), 3.75 (q, $(CH_3CH_2O)_3Si$–, 6), and 4.06 (q, –COO–CH_2–CH_3, 2).

3.2 Modification of P-NPs with S2E11

After the formation of P-NPs, due to the hydrolysis process, there were many hydroxyl groups (-OH) on the surface

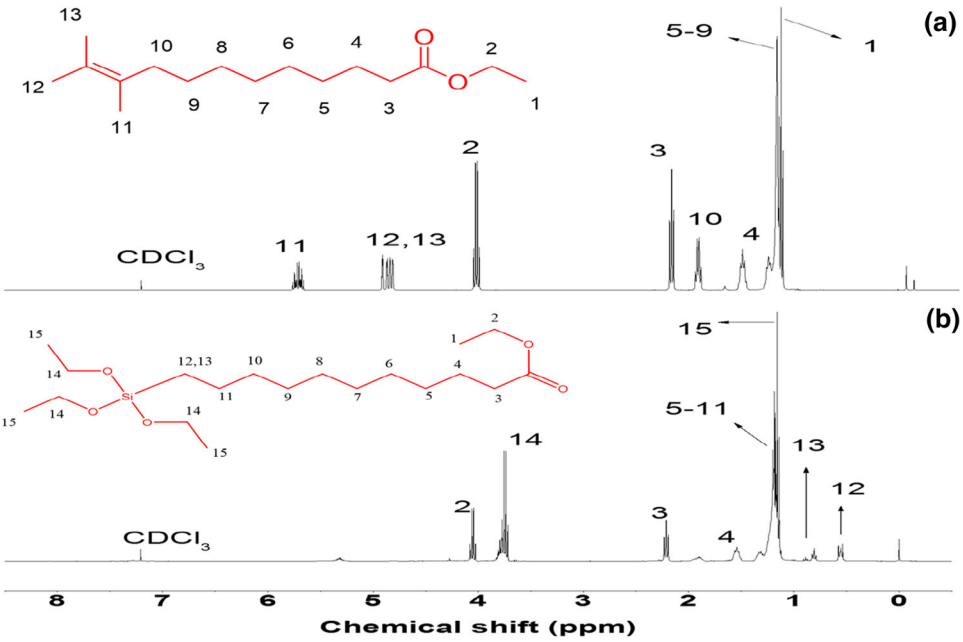

Fig. 1 ^{1}H-NMR spectra of **a** ethyl-10-undecenoate and **b** ethyl 11-(triethoxysilyl)undecanoate (hydrosilylation product)

of particles. The -Si-$(OC_2H_5)_3$ groups of S2E11 product were hydrolyzed in the solution and converted into hydroxyl groups (-OH) due to ammonium hydroxide base catalyst. These hydroxides get condensed with hydroxides of P-NPs through a hydrolytic condensation reaction. During this process, hexamethylenetetramine slowly converted into ammonia due to high temperature as sustained-release precipitant. This ammonia was further hydrolyzed to hydroxyl ions to promote the condensation process of S2E11 on the surface of P-NPs [18]. Finally, a core–shell structure was formed having a rigid core of silsesquioxane with a long carbon chain containing shell.

3.2.1 FTIR Analysis

The FTIR spectra of P-NPs, hydrosilylation product S2E11, and MP-NPs are shown in Fig. 2. The characteristic Si–O–Si linkages of P-NPs showed the signal at 1025 cm^{-1} (bending) and 1120 cm^{-1} (stretching), which was further confirmed by a discrete vibration at 442 cm^{-1} (bending). The C–H (stretching) frequency of all three materials appeared at 2950 cm^{-1} while Si–C (stretching) at 760 cm^{-1} [19,20]. The C–H signal of Si-CH_3 at 1260 cm^{-1} also showed its presence in spectra. For MP-NPs, a significant peak of carbonyl carbon of ester group appeared at 1730 cm^{-1}, which clearly shows that long carbon chain containing ester group has been successfully modified on the surface of nanoparticles. [21]

3.2.2 SEM and EDS Analysis

After preparing the PMSQ nanoparticles by a single-step sol–gel process, they were analyzed by SEM. The SEM

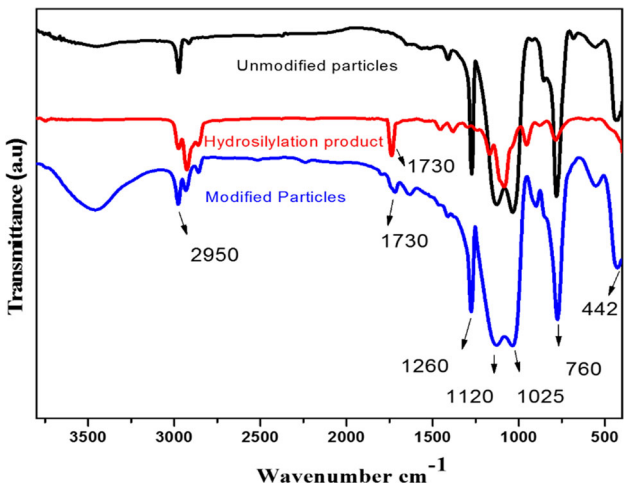

Fig. 2 FTIR spectra of P-NPs, hydrosilylation product S2E11, and MP-NPs

showed their morphology as spherical in shape, well separated, and in the range of 200–300 nm as shown in Fig. 3. The modification of P-NPs can be easily analyzed by SEM analysis as shown in Fig. 3 (with magnification factors of SEM-8010 (Hitachi, Japan): Fig. 3a. SU8010 1.5 kV 9.9mmx60.0 k SE(UL) and Fig. 3b. SU8010 1.5 kV 4.9 mm x 60.0 k SE(UL).

It shows that the surface of P-NPs is neat, whereas the surface of the MP-NPs is not neat, and we cannot see the bare surface of P-NPs. This phenomenon indicates that the long carbon chain containing S2E11 has been successfully grafted on the surface of P-NPs and the result is consistent with elemental analysis (EDS data) [22]. The EDS data in

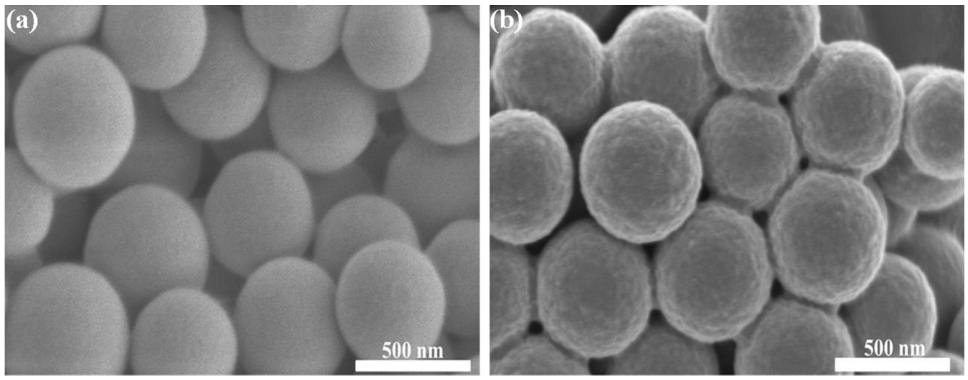

Fig. 3 SEM images of **a** P-NPs and **b** MP-NPs

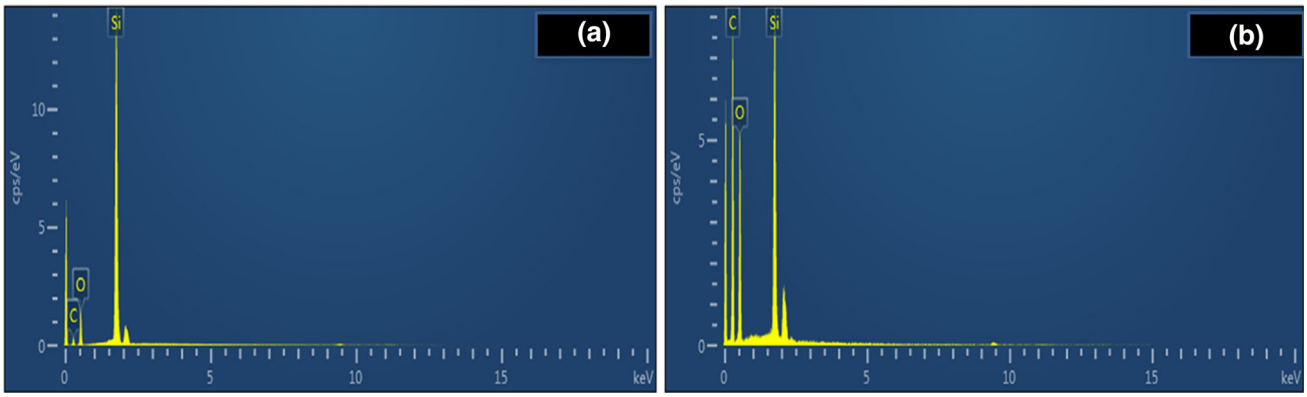

Fig. 4 EDS analysis of **a** P-NPs and **b** MP-NPs

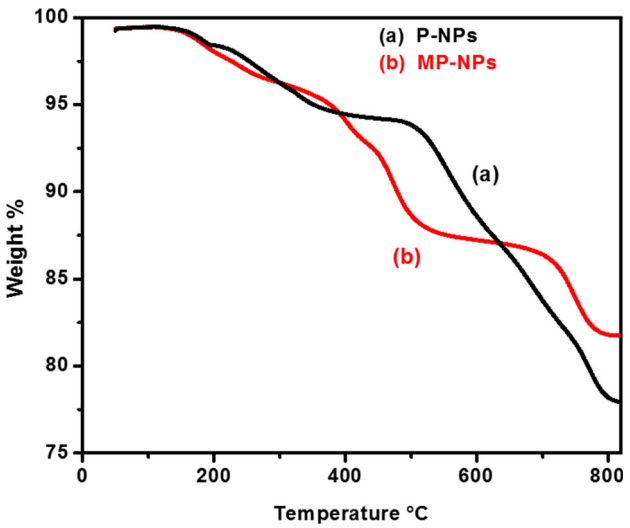

Fig. 5 TGA curves of **a** P-NPs and **b** MP-NPs

Fig. 4 show the percentage of elements in P-NPs before and after modification.

It reveals that before modification the weight percentage of carbon and oxygen (C = 20.73% and O = 22.34%) was low but after modification due to the involvement of long carbon chains of ethyl 10-undecenoate, the percentage of carbon and oxygen (C = 40.21% and O = 33.63%) has increased that shows the incorporation of S2E11 on the surface of P-NPs. However, this EDS also shows the absence of fluorine in both P-NPs and MP-NPs.

Table 1 TGA data for P-NPs and MP-NPs

Samples	T_5/ °C	T_{10}/ °C
P-NPs	344.03	566.96
MP-NPs	384.81	486.79

3.2.3 TGA Analysis

The TGA curves of P-NPs and MP-NPs under N_2 atmosphere are shown in Fig. 5. Here, T_5 and T_{10} are the temperatures at which 5% and 10% weight losses have occurred, respectively, which are summarized in Table 1.

The 5% and 10% weight losses of P-NPs are 344.03 °C and 566.96 °C which is a much higher temperature than 384.81 °C and 486.79 °C of MP-NPs, respectively. This indicates the P-NPs has been successfully modified with the long carbon chains of S2E11 due to which 10% weight loss occurred at a lower temperature than P-NPs and showed higher thermal stability.

The thermogravimetric analysis revealed that our long carbon chain containing nanolubricant additive has extraordinary thermal stability than other lubricant additives as the

Table 2 Thermal stability comparison of MP-NPs with other lubricant additives

Sr. no.	Weight loss (%)	[a]Described temp. (°C)	Material	Reference
1	19	800	MP-NPs	This work
2	35	800	[b]RGO-g-OA	[30]
3	72	600	[c]PBS/BCL	[31]
4	79.2	700	[d]OD-POSS	[7]
5	90	400	[e]CDs-NTf2/PEG	[32]

[a]The final temperature described in the relevant article. [b]Reduced graphene oxide grafted on octadecyl alcohol. [c] PBS/BCL poly(butylenes succinate) with bamboo carbon lubricant 50% wt. Content.[d]1-octadecanethiol with polyhedral oligomeric silsesquioxanes. [e]Capped carbon dots with NTf2 in polyethylene glycol

Table 3 Tribological testing conditions

Parameters	Description
Module	Four balls: upper one ball was rotatable; lower three balls were stationary
Steel balls	GCr 15
Applied load	250 N
Rotational speed	400 rpm
Test time	30 min for each, every sample was tested 3 times
Lubricant oil (base oil) Lubricant additive	Silicone oil. 50 g in each sample P-NPs with 0, 0.05, 0.1, 0.3, 0.5 wt% and MP-NPs with 0, 0.05, 0.1, 0.3, 0.5 wt%
Atmosphere	Room temperature, air

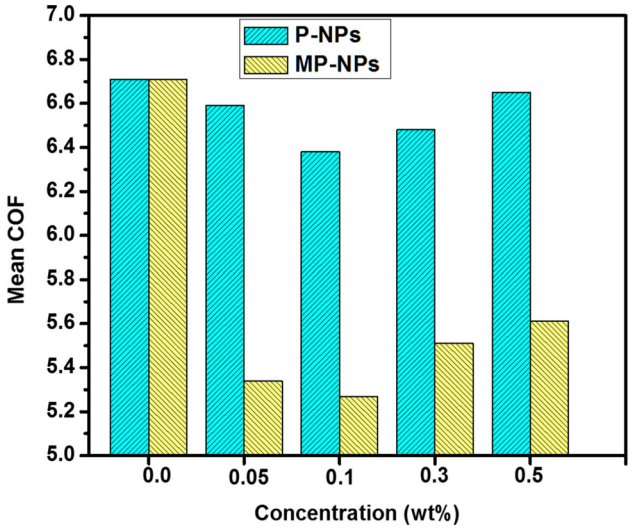

Fig. 6 Mean coefficient-of-friction (COF) values of steel balls lubricated with the mixture of silicone oil and P-NPs and that of silicone oil and MP-NPs at different concentrations

comparison shown in Table 2. The final weight % loss of MP-NPs is merely 19% even at 800 °C, while all other lubricant additives have much lower thermal stability. The support of robust and compact Si–O–Si three-dimensional network made the long carbon chain containing nanoparticles a unique type of amazingly thermally stable material that can be preferably used in heavy machinery, metal wire drawing, and those industries where harsh conditions are employed and high thermally stable materials are required that can withstand the high temperature [23].

4 Tribological Performance

In our research, the silicone oil was purchased from Sino Chemical Reagents and used as a base oil for tribological tests. The tribological properties of the steel balls sliding pairs lubricated with various concentrations of P-NPs and MP-NPs in silicone oil were investigated by Natai four-ball friction machine. The friction testing parameters are given in Table 3.

In order to investigate the tribological performance of P-NPs and MP-NPs in silicone oil, the different mixtures were mechanically stirred for 30 min.; after that, they were subjected to ultrasonication at 50 °C for 30 min to gain better dispersion of particles. Figure 6 shows that when P-NPs were added into the silicone oil, the COF first decreased a little (from 6.71 to 6.64) but after that, these values got increased (from 6.64 to 6.69) by adding more amount of P-NPs from 0.0 to 0.5 wt %. In the same way, the WSD values of the steel balls also showed the similar behavior, as they also first decreased (from 0.469 to 0.464 mm) and then increased (0.464 to 0.467 mm) corresponding to the P-NPs from 0.0 to 0.5 wt% as shown in Fig. 7. This trend indicates that on average the performance of P-NPs was not good because of their higher amount; it may result in a slight decrease in the mixture's viscosity, which is not good for reducing the friction coefficient. Due to this phenomenon, the steel balls experienced more face-to-face surface contact that resulted in their abrasiveness and hence increase in their WSD values [24].

These frictional changes can be partly supported and evident by the used amount of P-NPs with the help of surface elemental analysis EDS data that show the increasing weight percentage of C from 10.44, 11.27, 13.53, 16.43 to 19.82% by adding the concentration of P-NPs from 0, 0.05, 0.1, 0.3,

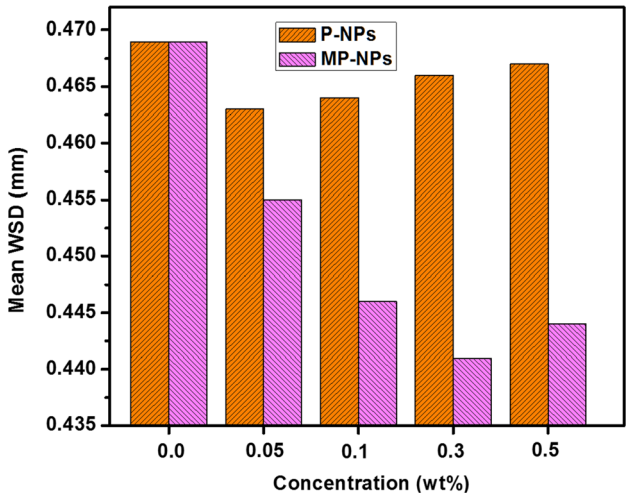

Fig. 7 Mean wear scar diameter (WSD) and coefficient-of-friction (COF) values of steel balls lubricated with a mixture of silicone oil and P-NPs and that of silicone oil and MP-NPs at different concentrations

and 0.5 wt%, respectively, as shown in Figure S1a supporting information.

For evaluating the performance of MP-NPs, the silicone oil (base oil) was mixed with different concentrations of MP-NPs from 0, 0.05, 0.1, 0.3, and 0.5 wt%. Figure 6 shows that overall by adding MP-NPs up to 0.5 wt%, the COF decreased from 6.71 to 5.61. The maximum reduction was at 0.1 wt% (COF value 5.27), which is 20.56% as compared to pure silicone oil (COF value 6.71). After the optimal concentration of 0.1 wt% of MP-NPs, the COF slightly increases from 5.27 to 5.61 with an increase in additive concentration from 0.1 to 0.5 wt%, respectively. Due to the nanosize of PMSQ particles, this material possesses a large surface area and can form a lubrication layer on the frictional surface. An optimized and fine protective film formed on the frictional surface when the concentration of MP-NPs reaches up to 0.1 wt%, which protects the steel balls from direct contact and improves the tribological properties. But the successive increase in additive concentration in base oil leads to the random aggregation of the nanoparticles on the surface of steel balls that result in the slight increase in COF, which is not in favor to improve the friction performance of the system [7]. However, the WSD values of steel balls continuously decreased from 0.469 to 0.441 mm corresponding to the concentration of MP-NPs from 0.0 to 0.3 wt% with a little increase at 0.5 wt% (0.445 mm) as shown in Fig. 7.

The used amount of MP-NPs can be evident by EDS data that showed the increasing weight percentage of C from 10.44, 20.19, 22.93, 24.77, and 25.82% by adding the corresponding amount of MP-NPs from 0, 0.05, 0.1, 0.3, and 0.5 wt% as shown in Figure S1b supporting information. This trend indicates that on average the performance of MP-NPs is much better than P-NPs regarding both tribological parameters, COF and WSD. This is possibly due to the flexible long carbon chains on the surface of MP-NPs that form three-dimensional core–shell-based dendrimer-like structures. As compared with other commonly used solid lubricants, i.e., WS_2, MoS_2, TiO_2, and GO, these nanoparticles also comprise good dispersion and better organic compatibility [2,8,9]. Moreover, the rigid inorganic Si–O-Si core possesses the good thermal stability that makes these MP-NPs a good material to be used as a nanolubricant additive for improving the tribological properties [25].

This surface coating and friction improvement behavior can be imagined by an illustration diagram. Figure 8a shows the magnified surface of steel balls that interact with each other face to face. Here, in Fig. 8b, the MP-NPs are considered as tiny capsules impregnated with long carbon chains. When the upper steel ball rotates on lower balls after every rotation, the peaks and grooves at the nano- and microscale on the frictional surfaces directly contact with each other. The spherical silsesquioxanes act like small ball bearings that help to convert the sliding friction of steel balls into rolling friction. Due to the nanosize and large surface area, these particles help in self-repairing of the abrasive surface by filling the nano- and microscratches and form a smooth lubrication film on the steel balls in the friction process as shown in Fig. 8c.

5 Superhydrophobicity and Self-cleaning Property

Hydrophobicity is the combination of the nature of the material and its surface roughness. Hydrophobic materials are usually made of low-surface-energy-containing fluorine compounds or long carbon chains [26,27]. The MP-NPs have all these characteristics as they are fluorine-free (no harmful fluorine compounds as mentioned in heading 1, ref. [16,17,28,]) and have long carbon chains and rough surface. The wettability of MP-NPs embedded on the surface of glass by RTV binder was studied by Data Physics OCA 20 using the sessile drop technique. A 5 uL drop of deionized water was dropped on the bare glass, glass + RTV, and glass + RTV + MP-NPs as shown in Fig. 9.

From the water contact angle, it is obvious that the MP-NPs' layer showed Cassie–Baxter superhydrophobic behavior CA $= 151 \pm 3.4^{o}$, while bare glass and glass + RTV showed 58 ± 1.4^{o} and $101 \pm 2.1^{\circ}$, respectively. This phenomenon arises due to low-surface-energy-bearing long carbon chains and their rough surface. Due to the nonpolar nature of the long carbon chain, the water adhesion force was low at room temperature as depicted in Fig. 10, which shows that water droplets did not adhere to the superhydrophobic layer easily.

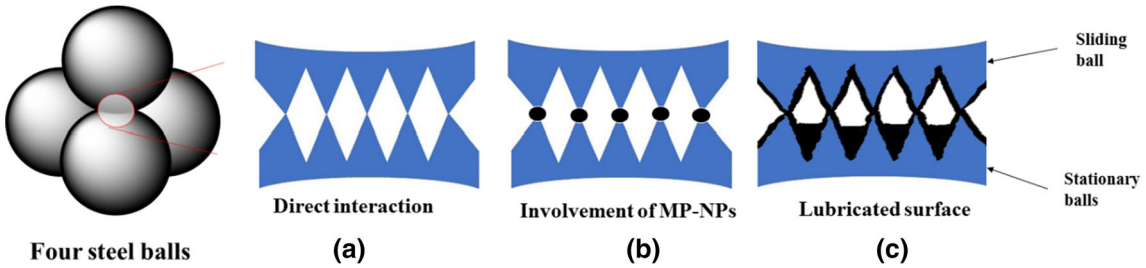

Fig. 8 An illustration diagram of MP-NPs improving the frictional performance

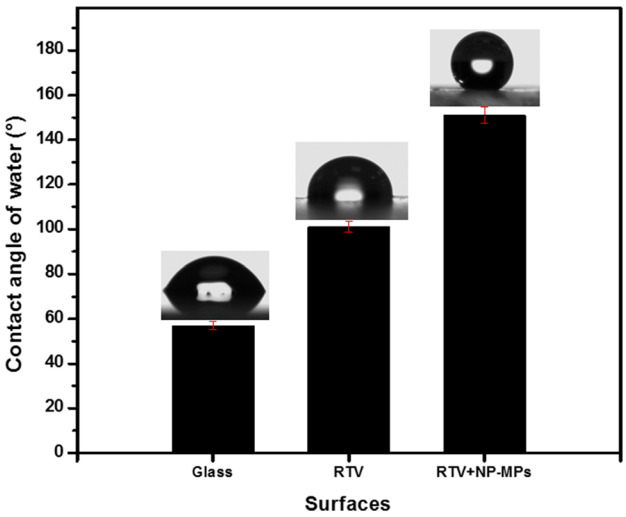

Fig. 9 Average water contact angles of **a** bare glass, **b** glass + RTV, and **c** glass + RTV + MP-NPs

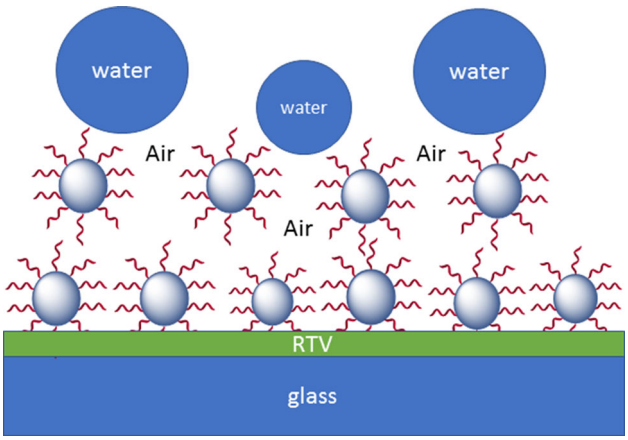

Fig. 10 Schematic description of trapped air among MP-NPs (superhydrophobic layer)

The surface roughness of superhydrophobic surfaces was discussed by Cassie et al. [29] in Eq. 1, which shows the effect of air gaps on the surface:

$$\cos\theta' = f_1\cos\theta_1 + f_2\cos\theta_2 \quad (1)$$

Here, θ‘ is the contact angle of a rough surface with trapped air. It is equal to the sum of contact angle of the solid–water surface with their fraction of surface area f_1 and contact angle of water–air θ_2 with their fraction of surface area f_2. The material used in this study has low-surface-energy long carbon chains and interspaces among them where the air resides or traps and gives a push-up effect to water; on this behalf, it can be said that these factors resulted as superhydrophobicity of MP-NPs as shown in Fig. 10.

As the long carbon chain containing surfaces repel the water drops and show low adhesion behavior, in the same way, our material showed the water roll of phenomenon at 25 °C [27]. We applied the water drop and pressed it but it did not attach with surface easily and showed very low adhesion with MP-NPs' layer as shown in Fig. 11. This implies that the nonpolar long carbon chain did not show the attraction for polar water droplets. So, the nonpolar nature of the surface and trapped air among its nanoparticles, together are responsible for this very low water adhesion.

All the characteristics of MP-NPs (i.e., nonpolar long carbon chains, rough surface behavior due to air gaps, low surface energy, and low water adhesion force) also gave rise to the surface self-cleaning performance. To examine this, sand particles (as dust) were placed on the glass slide coated with RTV + MP-NPs and a bare glass slide. As in video S1 supporting information, when the water drops touched sand on bare glass, they remained on the surface with sand and could not clean the surface while the drops when encountered with the modified glass surface swept away the dust particles and cleaned it easily.

6 Conclusion

The novel, economic, and captivating approach has been made to prepare long carbon chain containing PMSQ nanoparticles by condensation reaction followed by hydrosilylation product. As a unique type of proficient additive, these nanoparticles proved as an effective hybrid material to improve the tribological properties at low concentration with extraordinary thermal stability. The MP-NPs success-

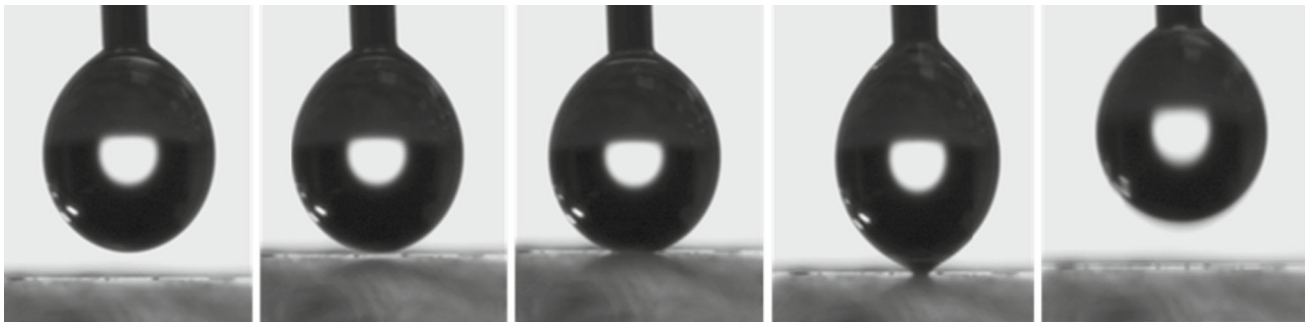

Fig. 11 A schematic view of very low water adhesion force of MP-NPs (glass + RTV + MP-NPs)

fully reduced the COF and WSD values up to 5.27 and 0.441 mm as compared to non-additive silicone oil of 6.71 and 0.469 mm, respectively. The total weight loss of MP-NPs was only 19% which makes this material workable in harsh conditions as compared to other solid lubricant additives. Additionally, these MP-NPs showed outstanding water repellency with CA 151°, i.e., superhydrophobicity, low water adhesion, and self-cleaning properties after embedded on glass with RTV binder. The SEM, EDS, and tribological analysis confirmed their efficiency as a good lubricant additive and OCA verified their environment-friendly (fluorine-free) superhydrophobicity. On these bases, it can be expected that these PMSQ hybrid nanoparticles can be further modified by other longer carbon chains and better applications can be achieved.

Acknowledgements C. Bittencourt is a Research Associate of the National Funds for Scientific Research (FRS-FNRS, Belgium). This work is partially supported by the MOST-WBI International Cooperation Project: the National Key R&D Programmes of China (No. 2017YFE0116000). The authors thank Dr. Jijiang Hu, Na Zheng, Li Xu, Sudan Shen, Jing He, Huibo Zhang, Qun Pu, and Eryuan Fang for their assistance in the analysis at State Key Laboratory of Chemical Engineering (Zhejiang University).

Compliance with ethical standards

Conflict of interest There is no conflict of interest related to this research.

References

1. Kim, K.-S.; Lee, H.-J.; Lee, C.; Lee, S.-K.; Jang, H.; Ahn, J.-H.; Kim, J.-H.; Lee, H.-J.: Chemical vapor deposition-grown graphene: the thinnest solid lubricant. ACS Nano **5**, 5107–5114 (2011). https://doi.org/10.1021/nn2011865
2. Wu, L.; Xie, Z.; Gu, L.; Song, B.; Wang, L.: Investigation of the tribological behavior of graphene oxide nanoplates as lubricant additives for ceramic/steel contact. Tribol. Int. **128**, 113–120 (2018). https://doi.org/10.1016/j.triboint.2018.07.027
3. Sliney, H.E.: Solid lubricant materials for high temperatures-a review. Tribol. Int. **15**, 303–315 (1982). https://doi.org/10.1016/0301-679X(82)90089-5
4. Shylesh, S.; Gokhale, A.A.; Ho, C.R.; Bell, A.T.: Novel Strategies for the Production of Fuels, Lubricants, and Chemicals from Biomass. Acc. Chem. Res. **50**, 2589–2597 (2017). https://doi.org/10.1021/acs.accounts.7b00354
5. Wang, L.; Xu, Z.; Wang, W.; Bai, X.: Atomic Mechanism of Dynamic Electrochemical Lithiation Processes of MoS $_2$ Nanosheets. J. Am. Chem. Soc. **136**, 6693–6697 (2014). https://doi.org/10.1021/ja501686w
6. Scharf, T.W.; Prasad, S.V.: Solid lubricants: a review. J. Mater. Sci. **48**, 511–531 (2013). https://doi.org/10.1007/s10853-012-7038-2
7. Liu, L.; Liu, Z.; Huang, P.: Novel POSS based nanohybrids for improving tribological properties of liquid paraffin. RSC Adv. **6**, 94876–94883 (2016). https://doi.org/10.1039/c6ra21618h
8. Lu, Z.; Cao, Z.; Hu, E.; Hu, K.; Hu, X.: Preparation and tribological properties of WS<inf>2</inf>and WS<inf>2</inf>/TiO<inf>2</inf>nanoparticles. Tribol. Int. **130**, 308–316 (2019). https://doi.org/10.1016/j.triboint.2018.09.030
9. Simić, D.; Stojanović, D.B.; Kojović, A.; Dimić, M.; Totovski, L.; Uskoković, P.S.; Aleksić, R.: Inorganic fullerene-like IF-WS2/PVB nanocomposites of improved thermo-mechanical and tribological properties. Mater. Chem. Phys. **184**, 335–344 (2016). https://doi.org/10.1016/j.matchemphys.2016.09.060
10. Mihelčič, M.; Gaberšček, M.; Di Carlo, G.; Giuliani, C.; Salzano de Luna, M.; Lavorgna, M.; Surca, A.K.: Influence of silsesquioxane addition on polyurethane-based protective coatings for bronze surfaces. Appl. Surf. Sci. 467–468, 912–925 (2019). https://doi.org/10.1016/j.apsusc.2018.10.217
11. Ahmed, N.; Fan, H.; Dubois, P.; Zhang, X.; Fahad, S.; Aziz, T.; Wan, J.: Nano-engineering and micromolecular science of polysilsesquioxane materials and their emerging applications. J. Mater. Chem. A. (2019). https://doi.org/10.1039/C9TA04575A
12. Du, X.; Kleitz, F.; Li, X.; Huang, H.; Zhang, X.; Qiao, S.Z.: Disulfide-bridged organosilica frameworks: designed, synthesis, redox-triggered biodegradation, and nanobiomedical applications. Adv. Funct. Mater. (2018). https://doi.org/10.1002/adfm.201707325
13. Quang, D.V.; Dindi, A.; Al-Ali, K.; Abu-Zahra, M.R.M.: Template-free amine-bridged silsesquioxane with dangling amino groups and its CO2 adsorption performance. J. Mater. Chem. A. **6**, 23690–23702 (2018). https://doi.org/10.1039/c8ta05106b
14. Ivanova, N.A.; Zaretskaya, A.K.: Simple treatment of cotton textile to impart high water repellent properties. Appl. Surf. Sci. **257**, 1800–1803 (2010). https://doi.org/10.1016/j.apsusc.2010.09.021
15. Huo, L.; Du, P.; Zhou, H.; Zhang, K.; Liu, P.: Fabrication and tribological properties of self-assembled monolayer of n-alkyltrimethoxysilane on silicon: effect of SAM alkyl chain length. Appl. Surf. Sci. **396**, 865–869 (2017). https://doi.org/10.1016/j.apsusc.2016.11.049

16. Yeung, L.W.Y.; De Silva, A.O.; Loi, E.I.H.; Marvin, C.H.; Taniyasu, S.; Yamashita, N.; Mabury, S.A.; Muir, D.C.G.; Lam, P.K.S.: Perfluoroalkyl substances and extractable organic fluorine in surface sediments and cores from Lake Ontario. Environ. Int. **59**, 389–397 (2013). https://doi.org/10.1016/j.envint.2013.06.026
17. Wang, Z.; Cousins, I.T.; Scheringer, M.; Buck, R.C.; Hungerbühler, K.: Global emission inventories for C4-C14 perfluoroalkyl carboxylic acid (PFCA) homologues from 1951 to 2030, part II: The remaining pieces of the puzzle. Environ. Int. **69**, 166–176 (2014). https://doi.org/10.1016/j.envint.2014.04.006
18. Yuan, J.; Ma, W.; Mo, J.: Fabrication of highly monodisperse CeO2@poly(methyl silsesquioxane) microspheres and their application in UV-shielding films. J. Appl. Polym. Sci. (2017). https://doi.org/10.1002/app.45065
19. Husamelden, E.; Fan, H.: Fluorinated functionalization of graphene oxide and its role as a reinforcement in epoxy composites. J. Polym. Res. (2019). https://doi.org/10.1007/s10965-018-1687-z
20. Zhang, X.; Ma, Z.; Fan, H.; Bittencourt, C.; Wan, J.; Dubois, P.: A novel polyhedral oligomeric silsesquioxane-modified layered double hydroxide: preparation, characterization and properties. Beilstein J. Nanotechnol. **9**, 3053–3068 (2018). https://doi.org/10.3762/bjnano.9.284
21. Ullah, R.S.; Wang, L.; Yu, H.; Haroon, M.; Elshaarani, T.; Naveed K. ur, S.; Fahad, S.; Khan, A.; Nazir, A.; Xia, X.; Teng, L.: Synthesis of polyphosphazene and preparation of microspheres from polyphosphazene blends with PMMA for drug combination therapy. J. Mater. Sci. **54**, 745–764 (2019). https://doi.org/10.1007/s10853-018-2843-x
22. Shirgholami, M.A.; Shateri Khalil-Abad, M.; Khajavi, R.; Yazdanshenas, M.E.: Fabrication of superhydrophobic polymethylsilsesquioxane nanostructures on cotton textiles by a solution-immersion process. J. Colloid Interface Sci. **359**, 530–535 (2011). https://doi.org/10.1016/j.jcis.2011.04.031
23. Lu, X.; Yin, Q.; Xin, Z.; Li, Y.; Han, T.: Synthesis of poly(aminopropyl/methyl)silsesquioxane particles as effective Cu(II) and Pb(II) adsorbents. J. Hazard. Mater. **196**, 234–241 (2011). https://doi.org/10.1016/j.jhazmat.2011.09.020
24. Yang, F.; Yao, B.; Li, C.; Sun, G.; Ma, X.: Oil dispersible polymethylsilsesquioxane (PMSQ) microspheres improve the flow behavior of waxy crude oil through spacial hindrance effect. Fuel **199**, 4–13 (2017). https://doi.org/10.1016/j.fuel.2017.02.062
25. Bhushan, B.; Palacio, M.; Schricker, S.: Effect of polyhedral oligomeric silsesquioxane concentration on the friction and wear of dental polymers. J. Vac. Sci. Technol. A Vacuum Surf. Film **28**, 713–718 (2010). https://doi.org/10.1116/1.3299103
26. Jamil, M.I.; Ali, A.; Haq, F.; Zhang, Q.; Zhan, X.; Chen, F.: Icephobic strategies and materials with superwettability: design principles and mechanism. Langmuir **34**, 15425–15444 (2018). https://doi.org/10.1021/acs.langmuir.8b03276
27. Jamil, M.I.; Zhan, X.; Chen, F.; Cheng, D.; Zhang, Q.: Durable and scalable candle soot icephobic coating with nucleation and fracture mechanism. ACS Appl. Mater. Interfaces. **11**, 31532–31542 (2019). https://doi.org/10.1021/acsami.9b09819
28. Lu, Z.; Song, L.; Zhao, Z.; Ma, Y.; Wang, J.; Yang, H.; Ma, H.; Cai, M.; Codling, G.; Ebinghaus, R.; Xie, Z.; Giesy, J.P.: Occurrence and trends in concentrations of perfluoroalkyl substances (PFASs) in surface waters of eastern China. Chemosphere **119**, 820–827 (2015). https://doi.org/10.1016/j.chemosphere.2014.08.045
29. Cassie, A.B.D.: Contact angles. Discuss. Faraday Soc. **3**, 11–16 (1948). https://doi.org/10.1039/DF9480300011
30. Zhu, C.; Yan, Y.; Wang, F.; Cui, J.; Zhao, S.; Gao, A.; Zhang, G.: Facile fabrication of long-chain alkyl functionalized ultrafine reduced graphene oxide nanocomposites for enhanced tribological performance. RSC Adv. **9**, 7324–7333 (2019). https://doi.org/10.1039/c9ra00433e
31. Huang, S.; Pan, B.; Wang, Q.: Study on the hardness and wear behavior of eco-friendly Poly(butylenes Succinate)-based bamboo carbon composites. Arab. J. Sci. Eng. **44**, 7997–8003 (2019). https://doi.org/10.1007/s13369-019-04002-6
32. Wang, B.; Tang, W.; Lu, H.; Huang, Z.: Ionic liquid capped carbon dots as a high-performance friction-reducing and antiwear additive for poly(ethylene glycol). J. Mater. Chem. A. **4**, 7257–7265 (2016). https://doi.org/10.1039/c6ta01098a